

A new hardware-in-the-loop platform for the evaluation of adaptive lighting systems

A. Opfermann* , T. Bertram* , D. Baum** and P. Karas**

* *Chair for Control Systems Engineering, Faculty of Electrical Engineering and Information Technology, Universität Dortmund, D-44221 Dortmund, Germany (Tel: +49/231/755-3592; e-mail: alexander.opfermann@uni-dortmund.de),*

** *Hella KGaA Hueck & Co., D-59555 Lippstadt, Germany.*

Abstract: In this paper a new hardware-in-the-loop platform for the evaluation of adaptive lighting systems is presented. A standard industrial robot is actuated with input data from a vehicle dynamics simulation in order to position a pair of active frontlighting headlamps mounted at the tool center point. With this setup test drives can be simulated repeatedly under well-defined environmental conditions at any time. A visual measurement system is presented that tracks the dynamic light distribution and thus provides data that can be related to subjective impressions by means of statistical analysis tools.

Keywords: adaptive systems; automatic testing; automotive; cameras; dynamic behaviour; evaluation; light; robotic manipulators; vehicle dynamics.

1. INTRODUCTION

With the development of active frontlighting systems headlamps with a set of fixed switchable light distributions are more and more replaced by headlamps with additional degrees of freedom, allowing the lighting system to automatically adjust the light distribution to the traffic scenario, the roads horizontal, and vertical curvature, the weather conditions, the vehicle dynamics and the drivers preferences. The industrial standard for active frontlighting systems are headlamps, that are rotated around their vertical (curve lighting) and horizontal (dynamic headlamp leveling) axes, that include fixed axle auxiliary light sources for situation-dependent activation and a variable aperture (town light, country light, motorway light, etc.).

The design procedure for static or dynamic light distributions is treated as an optimization problem with constraints given by legal requirements. This context results in an inherent necessity for continuously monitoring the operation and verification of the constraints. The latter is rather simple for the static case, since it only requires checking if certain thresholds for the illuminance values on a standardized projection surface are met, which is typically done in a laboratory experiment with a goniometer. For dynamic light distributions no established methods exist for constraint violation checking since the measurement of light distribution properties during driving maneuvers is difficult and strongly influenced by environmental factors such as the ambient light intensity or the weather conditions. Evaluating the quality in static and dynamic situations is even more challenging since this requires to relate the human visual perception with the light distribution properties in addition to measuring the latter. For reasons of practicability the evaluation is usually done by professional lighting engineers during night drives on spe-

cific test tracks with carefully selected maneuvers. Their experience is often the only measure of quality.

Various attempts have been considered to overcome the disadvantages like poor comparability, reproducibility or accuracy that are associated with subjective tests. The first alternative for benchmarking headlamps is to use a room with no ambient light and of appropriate dimensions for projecting the light distribution on the floor. Hence the evaluation is independent of external influences. However due to lack of space only static situations are compared.

With the development of fast computers as a second alternative simulation tools were derived, which include the most important, optically effective modules of the headlamp and which calculate the resulting quantities like luminous flux, illuminance, luminous intensity or luminance given a model of the illuminated surroundings [Wördenweber et al., 2007]. In the beginning these simulations were mainly used to see the effect of constructive changes in the shape of the headlamp reflector surface or other parts of the optical path on the static light distribution without manufacturing an expensive prototype of the headlamp [Lehnert, 2000]. More enhanced tools use these physically correct light distributions as part of a virtual reality simulation which allows the engineer to evaluate new headlamp designs under realistic conditions while driving in different scenarios. Further developed versions of these software tools include a sophisticated vehicle dynamics model and a software interface to other software development tools such as Matlab/Simulink so that headlamp function models are easily imported into the simulation for a direct evaluation. Nevertheless this approach neglects the mechanical properties of the adjustment mechanism and is only feasible if light distribution data and software models are available.

This paper presents the concept of a new hardware-in-the-loop (HIL) platform for the evaluation of automatic headlamps. It is composed of an industrial robot, a pair of automatic headlamps that is mounted to the robot, a vehicle dynamics simulation environment, that provides the input data to the robot as well as the headlamps, and a visual measurement system for tracking the dynamic light distribution. In the future it can be equipped with an adjustable mounting in order to evaluate and compare different types of headlamps easily and under constant test conditions. The method is independent from special software tools for lighting simulation and from external influences as well, since the setup is indoors. Furthermore the headlamp inclination is reconstructed by tracking the dynamic light distribution on a projection surface, so that it can be related to subjective evaluation. Finally all hardware and software components of the lighting system are accounted for, such that all relevant effects that potentially appear during test drives in a real car are also observed in the laboratory.

This paper is structured as follows: In section 2 and 3 the general idea and the previous system are described. In section 4 the application specific requirements concerning the headlamp motion in the vehicle are defined. Section 5 describes the mechanical setup of the selected robot together with the headlamp mounting and the overall system structure. In section 6 and 7 the concept of light distribution measurement with a camera and its transformation to virtual surfaces is described. The headlamp leveling algorithm as an example for an adaptive lighting system is presented in section 8 and tested with the new HIL system in section 9.

2. SYSTEM OVERVIEW

The aim of this concept is to bridge the gap between software-in-the-loop simulation and test drives in order to overcome the aforementioned disadvantages related to these types of evaluation. The concept is explained in figure 1. The main idea behind the test bench is that the

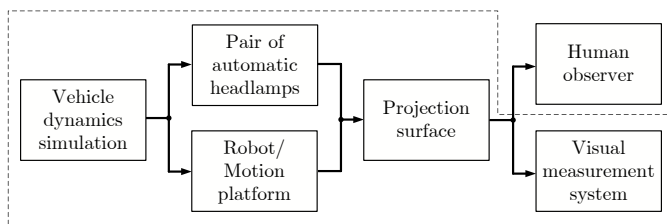


Fig. 1. Interdependence between system elements (dotted line denotes the elements considered in this paper)

forces transmitted from the lighting system to the car body can be neglected if the vehicle dynamics are concerned. Therefore the vehicle is substituted with a robot, which serves as a general purpose motion platform. The robot is actuated using motion data from a vehicle dynamics simulation that is carried out offline. A pair of automatic headlamps, which is mounted to the robot, is provided with further data from the same simulation experiment. The resulting motion of the light cone tip causes a dynamic light distribution on an arbitrary surface. The portion of light reflected from this surface is either observed by a subject or recorded with a visual measurement system.

3. PREVIOUS MOTION PLATFORM

The former system [Opgen-Rhein et al., 2003, Opgen-Rhein and Bertram, 2002] was developed at the Department of Mechatronics at the Gerhard-Mercator University in Duisburg during a project on the improvement of a dynamic headlamp leveling system. This setup has one degree of freedom so that only the pitch motion is realized. Figure 2 shows a front view together with the working principle. The position of the vehicle front end is adjusted according to the output of the vehicle dynamics simulation software FASIM C++ using a control loop comprising a linear actuator (Elero), an incremental encoder (Fritz Kuebler) and the realtime hardware MicroAutoBox (MAB, dSpace) as a controller. Since this concept is limited to a single degree of freedom and a narrow range of values for both angular displacement and angular velocity, alternatives have been examined.

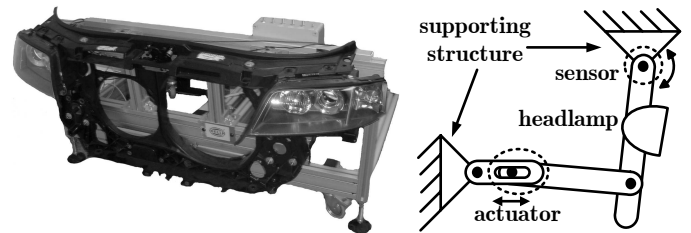


Fig. 2. Previous hardware-in-the-loop platform

4. OPERATING REQUIREMENTS

During the planing phase of the HIL system the overall objective was to reproduce the headlamp motion in the vehicle as accurate as possible. In the following the kinematic quantities related to the headlamp motion are described.

4.1 Degrees of freedom and coordinate systems

The headlamps are mounted stationary on the vehicle body (3) which is considered as a rigid body with three translational (x_B, y_B, z_B) (4, 5) and three rotational (ϕ_B, θ_B, ψ_B) degrees of freedom as shown in figure 3. For our application only the relative headlamp motion with respect to the coordinate system (x_R, y_R, z_R) (2), which resides halfway between both headlamps on the road surface is needed. Since the relative distances in lateral and longitudinal direction, as well as the relative orientation around the vertical axis remain constant, the quantities to be taken into account are the differences in vertical displacement $z_{HR/L} - z_R$, in roll angle $\phi_{HR/L} - \phi_R$ and in pitch angle $\theta_{HR/L} - \theta_R$. On a planar road the terms z_R, ϕ_R and θ_R are neglected.

4.2 Work space and dynamic ranges

For the previously defined quantities and their time derivatives the ranges of values are derived from typical ranges of values for the car body motion with respect to the road surface. Since only a rough estimate of the limits is needed, a vehicle simulation is the preferred costeffective evaluation method prior to real test drives. Applying extreme load situations, extreme suspension parameters

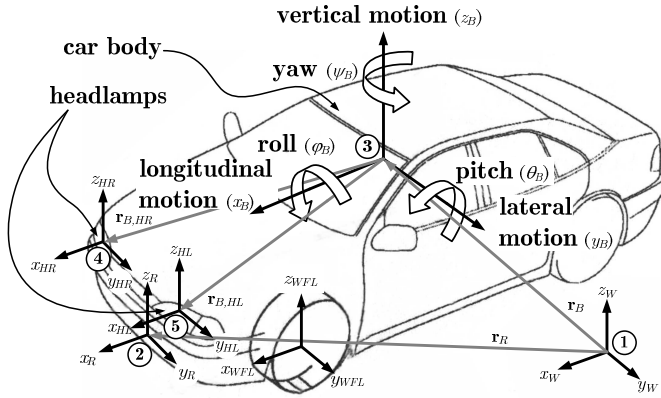


Fig. 3. Coordinate frames of road (1, 2), car body (3), and headlamps (4, 5)

and extreme driving maneuvers the bounds in table 1 are identified. These form the basis for the selection of a suitable motion platform.

Table 1. Dynamic ranges for headlamp motion

Quantity	[unit]	Lower bound	Upper bound
$z_{HL/R}$	[m]	0.5	0.8
$\phi_{HR/L}$	[°]	-10.0	10.0
$\theta_{HR/L}$	[°]	-5.0	5.0
$v_{z_{HL/R}}$	[m/s]	-0.4	0.4
$\omega_{\phi_{HR/L}}$	[°/s]	-40.0	40.0
$\omega_{\theta_{HR/L}}$	[°/s]	-7.5	-7.5

5. EXPERIMENTAL SETUP

The hardware components for testing new headlamp algorithms and their interactions are explained by figure 4, which gives a schematic overview. The central element is a personal computer (PC) with the vehicle dynamics simulation software IPG CarMaker, the rapid control prototyping software ControlDesk and Matlab/Simulink, which is interfaced by the other two programs.

IPG CarMaker comprises a parameterizable three-dimensional multibody vehicle model with 18 degrees of freedom. A road surface model is either build up from road segment primitives or imported. We import the road model from Matlab, so the road surface node coordinates are accessible for evaluation of light measurement quantities at these points. As the robot requires the cartesian positions and angles of the tool center point (TCP), a virtual kinematic sensor is fixed to the vehicle body at the relative position of the TCP to the headlamps. Running the simulation with a driver model gives the required signals from section 4.1 for the robot as well as additional signals such as the spring compression, the vehicle speed and the steering angle for the lighting algorithms.

The robot is connected to the PC through a 100MBit Ethernet network with a transmission control protocol/internet protocol (TCP/IP) and remotely controlled from Matlab using an advanced extensible markup language (XML) based interface. Position and orientation are updated every 10ms and set in cartesian space. For smooth

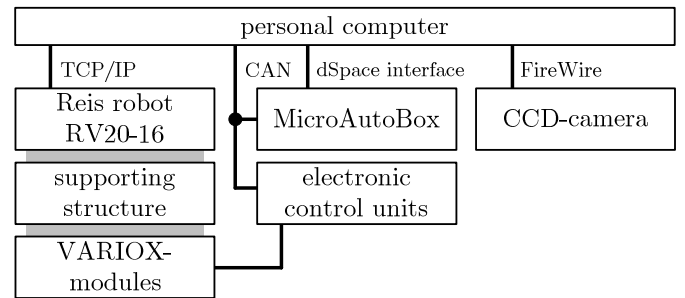
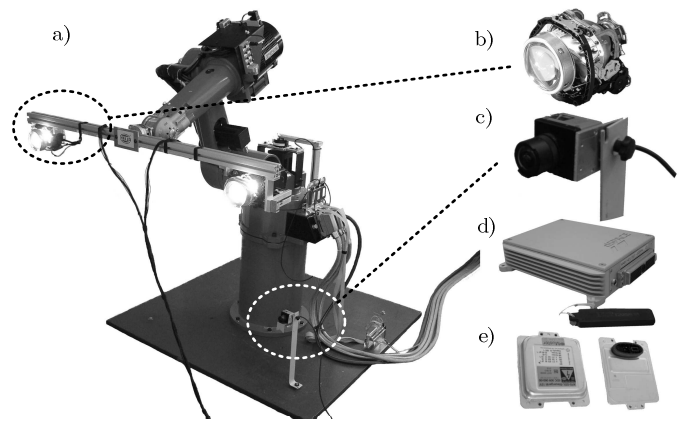


Fig. 4. New hardware-in-the-loop platform a) robot, b) projection module, c) charge coupled device (CCD) camera, d) MAB, e) electronic control units (ECU)

trajectories the robot moves in continuous path (CP) mode, i.e. it does not stop at each intermediate waypoint. A supporting structure is screwed to the TCP and carries two headlamp projection modules, is indicated by the gray bars.

ControlDesk provides a Simulink library with interface blocks used for connecting the MAB input and output ports to a Simulink model on the one hand and a graphical user interface to operate the box by remote control on the other hand. An automatic code generation procedure compiles the Simulink models into code that is then downloaded to the MAB through the dSpace interface. The MAB, a realtime rapid control prototyping hardware, runs the model with sampling times up to 1ms. Input signals for the lighting algorithm are sent from the PC to the MAB through a controller area network (CAN) using a USB-to-CAN-converter (Peak) that is accessible from Matlab. The electronic control units (ECU) are also part of the controller area network and run in bypass mode, so that the setpoint values received from the MAB are directly converted to power signals, that are sent to the headlamp projection modules. The new lighting algorithms can be tested quickly on the MAB.

The last component, a stationary CCD-camera (TheImagingSource DFK 21F04) with a monofocal lens (Computar T2616FICS-3), is mounted on an adjustable support beneath the robot base with its optical axis pointing towards the projection surface illuminated by the headlamps. It offers a resolution of 640x480 pixels at a frame rate of 30fps. It is connected to the PC by a FireWire interface. In the future it will be replaced by a special camera with a spectral sensitivity equal to the human eye.

6. CAMERA MODEL

The camera measures the photometric quantities on the projection surface. The relative positions of the camera and other elements of the experimental setup are displayed in figure 5. The coordinates of a point M_W in the base frame (robot base frame denoted by subscript W) on the illuminated surface and the illumination quantities at this point are derived separately. First the positions on the surface corresponding to the image pixels are found by the inverse mapping of a camera model. Then the photometric quantities at these points as well as at the headlamp positions and on the virtual surface are calculated with the laws of photometry.

A mapping of the point M_W into discrete image coordinates \mathbf{m} in the two-dimensional image plane is described by the perspective camera model [Schreer, 2005]

$$s\tilde{\mathbf{m}} = \mathbf{P}\tilde{M}_W, \quad \text{with } \mathbf{P} = \mathbf{A}\mathbf{P}_N\mathbf{D}, \quad (1)$$

where $\tilde{\cdot}$ denotes a vector in homogenous coordinates, \mathbf{P} is the general projection matrix and s is a scaling factor. The model subsumes an external, a perspective and an internal transformation in succession. The external transformation, which gives the point \tilde{M}_W in the camera frame (denoted by subscript C), is basically a rotation \mathbf{R} followed by a translation \mathbf{t} and is achieved by premultiplying with the homogeneous transformation matrix \mathbf{D}

$$\tilde{M}_C = \mathbf{D}\tilde{M}_W = [\mathbf{R} \ \mathbf{t}] \tilde{M}_W. \quad (2)$$

The perspective transformation maps a 3D point \tilde{M}_C in camera coordinates to its 2D projection $\tilde{\mathbf{m}}'$ in sensor coordinates by premultiplying it with the perspective projection matrix \mathbf{P}_N

$$\tilde{\mathbf{m}}' = \mathbf{P}_N \tilde{M}_C. \quad (3)$$

And finally the projected point $\tilde{\mathbf{m}}'$ is transferred to discrete image coordinates using the internal transformation and premultiplying with the intrinsic matrix \mathbf{A}

$$s\tilde{\mathbf{m}} = \mathbf{A}\tilde{\mathbf{m}}'. \quad (4)$$

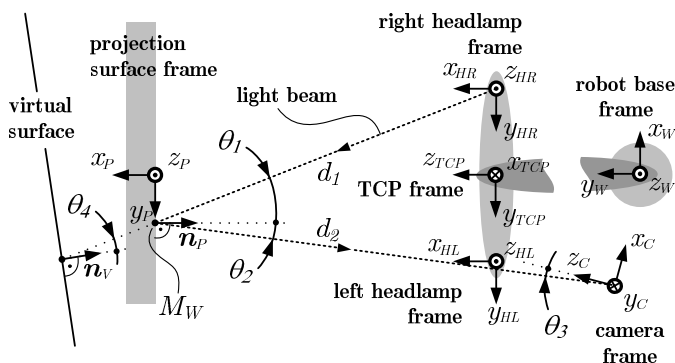


Fig. 5. Relative position of frames in top view

For camera calibration [Zhang, 1999] the Calib Toolbox for Matlab from the DLR is used. The calibration pattern is screwed to the TCP and presented to the camera in a

sequence of 20 poses taught in advance. As a result of calibration the extrinsic and intrinsic camera parameters are obtained. The position of the TCP in the robot base frame is derived from the robot axis angles using the direct kinematics. The position of the pattern frame is measured in the TCP frame. The extrinsic parameters, i.e. the relative position and orientation between the camera frame and the pattern frame, are different for each frame. For the absolute pose of the camera all sets of extrinsic parameters are transformed from pattern into world coordinates. After this an average set of extrinsic parameters is derived from all images.

Our application requires the computation of points on the projection surface corresponding to the discrete image coordinates. Therefore the inverse transformations to 2, 3 and 4 are performed. The normalized pixel positions in the 2D sensor coordinate system are derived by premultiplying with the inverse intrinsic matrix

$$\tilde{\mathbf{m}}' = \mathbf{A}^{-1}\tilde{\mathbf{m}}. \quad (5)$$

The point M_W on the projection surface is derived for each pixel separately. It lies on a line from the focal point C to the pixel position \mathbf{m}' in the distance d_2 to C

$$M_W = C + d_2 \frac{C - \mathbf{m}'}{|C - \mathbf{m}'|}. \quad (6)$$

Substituting 6 into the equation of the projection plane

$$\mathbf{n}_P(P - M_W) = 0, \quad (7)$$

gives the distance d_2 .

7. ILLUMINATION MODEL

The headlamps are assumed as point light sources moving in 3D-space with a nonuniform luminous intensity distribution $I(\phi, \gamma)$, with ϕ and θ being the azimuth and elevation angle respectively. The continuous distribution is approximated by pencils of light, which intersect with a projection surface at a certain point M_W at a distance d_1 under an angle of incidence θ_1 as illustrated in figure 5. For a single headlamp the illuminance E_P at M_W is given by the inverse square law

$$E_P = \frac{\cos \theta_1 I(\phi, \theta)}{d_1^2}. \quad (8)$$

According to the principal of superposition the total illuminance is the sum of both headlamp sources. The surface is supposed to be diffuse and the luminous emittance M_P , i.e. the luminous flux dF related to an infinitesimal surface element dA , is proportional to the illuminance E_P

$$M_P = \rho E_P, \quad (9)$$

with the albedo ρ as a loss factor, that accounts for the absorbed light energy. The brightness of a pixel is a measure for the illuminance E_C on the corresponding CCD-sensor surface element in the focal point. From the etendue the relation between E_C and M_P is derived

$$E_C = \frac{A_P \cos \theta_2 \cos \theta_3}{\pi d_2^2} M_P, \quad (10)$$

with the emitting area A_P , the angle of emergence θ_2 , the angle of incidence θ_3 with respect to the optical axis and the distance d_2 between M_C and C . With 8, 9, and 10 $I(\phi, \theta)$ is calculated from E_C . Since a photometer is not available so far, the constant gain due to camera sensitivity and albedo is calibrated with the average maximum illuminance of a Xenon headlamp which is 220lx. The problem of superposition is solved by a separate treatment of left and right headlamp. With 8 the illuminance E_V can be calculated on any virtual surface, for example a 25m-distant measurement screen or a road surface.

8. DYNAMIC HEADLAMP LEVELING

The headlamp is attached to the car body, such that its vertical position $z_{H,B}$ and pitch orientation $\theta_{H,B}$ with respect to a plane road are derived from the car body motion z_B and θ_B

$$z_{H,B} = z_B - l_H \theta_B, \quad \theta_{H,B} = \theta_B, \quad (11)$$

with l_H as the distance between the car body frame and the headlamp frame in longitudinal direction.

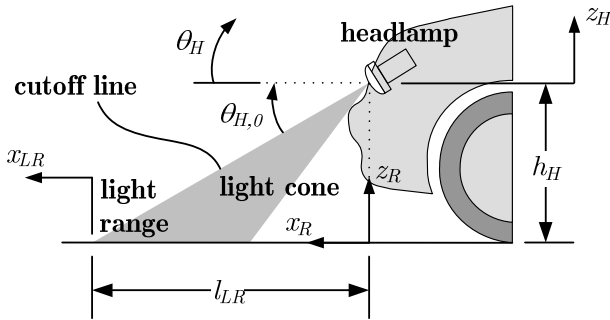


Fig. 6. Headlamp position and orientation and resulting cutoff line on the road

Since active headlamps possess an additional rotational degree of freedom $\theta_{H,COR}$ around the pitch axis, the resulting motion of the light cone tip is the superimposed motion of the car body and the active projection module at that position

$$z_H = z_{H,B}, \quad \theta_H = \theta_{H,B} + \theta_{H,COR}. \quad (12)$$

The required light range l_{LR} , i.e. the distance between the required cutoff line on the road surface and the headlamp position in x -direction, is calculated from the headlamp mounting point height h_H and the statutory cutoff line inclination $\theta_{H,0}$ using the tangent relation in the rectangular triangle (figure 6)

$$\theta_{H,0} = -\tan\left(\frac{h_H}{l_{LR}}\right), \quad l_{LR} = -\frac{h_H}{\arctan \theta_{H,0}}. \quad (13)$$

The actual range of light deviates from the required light range l_{LR} by the difference x_{LR} . This difference is further divided into a static and a dynamic part and is calculated as follows

$$x_{LR} + l_{LR} = -\frac{z_H}{\arctan \theta_H}, \quad (14)$$

$$x_{LR} = -\frac{z_H}{\arctan \theta_H} - l_{LR} \approx -\frac{z_H}{\theta_H} - l_{LR},$$

with $\arctan \theta_H \approx \theta_H$ for small θ_H .

8.1 Inclination angle setpoint

The objective of a headlamp leveling system is to minimize the difference x_{LR} . With this requirement an optimal correction angle $\theta_{H,OPT}$ for the rotation of the headlamp projection module is defined in terms of car body coordinates z_B and θ_B

$$0 \equiv -\frac{z_{H,B} + h_H}{\theta_{H,B} + \theta_{H,0} + \theta_{H,OPT}} - l_{LR}, \quad (15)$$

$$\theta_{H,OPT} = \frac{\theta_{H,0}}{h_H} z_{H,B} - \theta_{H,B} = \frac{\theta_{H,0}}{h_H} z_B - \left(1 + \frac{\theta_{H,0}}{h_H} l_H\right) \theta_B.$$

In typical headlamp leveling systems z_B and θ_B are not measured directly. Instead the spring deflections $z_{REL,F}$ and $z_{REL,R}$ at the front and the rear wheel suspensions respectively serve as input signals, since these are closely related to the car body motion and easy to measure. The vertical displacement $z_{H,ECU}$ and the rotation $\theta_{H,ECU}$ of the headlamp in terms of spring deflections are derived using intercept theorems

$$z_{H,ECU} = \frac{l_H - l}{l} (z_{REL,F} - z_{REL,R}) + z_{REL,F}, \quad (16)$$

$$\theta_{H,ECU} = \frac{z_{REL,R} - z_{REL,F}}{l}. \quad (17)$$

Introducing these approximations into equation 15 and substituting $z_{REL,F}$ and $z_{REL,R}$ by car body motion z_B and θ_B , and wheel mass motion $z_{W,F}$ and $z_{W,R}$ gives the correction angle calculated by the ECU

$$\theta_{H,ECU}^* = \frac{\theta_{H,0}}{h_H} z_B - \left(1 + \frac{\theta_{H,0}}{h_H} l_H\right) \theta_B + \quad (18)$$

$$+ \left(\frac{\theta_{H,0}}{h_H} \frac{l_H}{l} + \frac{1}{l}\right) z_{W,R} + \left(\frac{\theta_{H,0}}{h_H} \left(1 - \frac{l_H}{l}\right) - \frac{1}{l}\right) z_{W,F}.$$

It can be seen by comparison of 18 with 15 that both are equal up to the wheel motion terms $\theta_{H,ERR} = \theta_{H,ECU}^* - \theta_{H,OPT}$.

8.2 Setpoint filtering

The error $\theta_{H,ERR}$ is the reason for a second component inherent to all dynamic headlamp leveling systems of this working principle, namely a low pass filter

$$G_F(s) = \frac{Y(s)}{X(s)} = \frac{1}{1 + sT_F}, \quad (19)$$

with a time-variable filter time constant T_F . The time constant is reduced during the time period of transient car body motion due to acceleration and deceleration maneuvers, so the time delay between vehicle motion and headlamp reaction is minimized. During constant velocity drives it is increased to avoid headlamp motion resulting from road unevenness and thus minimize $\theta_{H,ERR}$.

A simple filter adaptation rule follows, if the input to the filter $x(t) = kt$ is assumed a ramp with slope k . Then the stationary difference $e_\infty = e(t)|_{t \rightarrow \infty} = y(t) - x(t)$ between filter output and input is equivalent to the product kT_F of slope and time constant. Therefore $T_{Fmax} = e_{max}/|k|$ is determined by the tolerable error due to filtering and the absolute input signal slope. The slope k is observed indirectly according to figure 7 under the assumption, that $x(t)$ is related to the input $u(t)$ of the system $G_S(s)$, which represents the vertical vehicle dynamics. The input $u(t)$ is the vehicle longitudinal Force $F_X = ma_X$. Its slope is estimated by using the second time derivative $\ddot{\omega}_{ij}$ of the wheel rotational velocity.

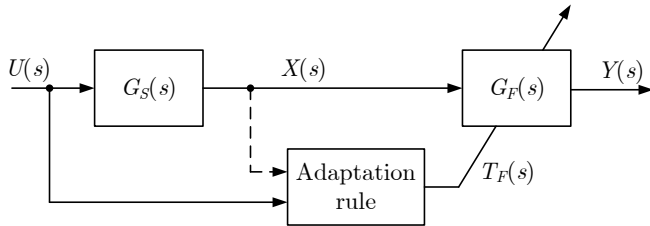


Fig. 7. Adaptation scheme of time-variable lowpass filter

9. EXPERIMENTAL RESULTS

For the evaluation of dynamic headlamp leveling systems the subjective visual impression of human observers have to be related to measurable quantities. These quantities are the headlamp motion $\theta_{H,B}$ and $z_{H,B}$ due to car body motion and the filtered inclination angle $\theta_{H,ECUF}$ of the headlamp relative to the vehicle body. $\theta_{H,B}$ and $z_{H,B}$ are known from vehicle simulation. The inclination angle is measured with a camera in order to avoid disassembling the headlamp for direct measurement. Nevertheless at this stage there is still an angular encoder mounted directly to the headlamp rotational axis in order to evaluate the performance of indirect inclination measurement using the camera. The following results show that $\theta_{H,ECUF}$ is reconstructed properly from the resulting dynamic light distribution on a projection surface observed by a stationary camera. The input signals to the robot and the headlamps are generated offline by simulating an acceleration-deceleration maneuver with IPG-CarMaker in advance. The vehicle speed and the spring deflections at the front and the rear suspensions are shown in figure 8.

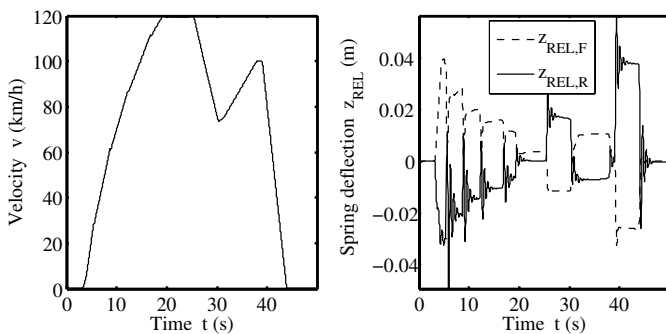


Fig. 8. Input signals from vehicle dynamics simulation

For this maneuver the dynamic light distribution on a projection surface in 4 meters distance to the headlamps

is observed by a camera. The camera picture is shown in figure 9 together with two markers representing the tracked points, one for each headlamp.

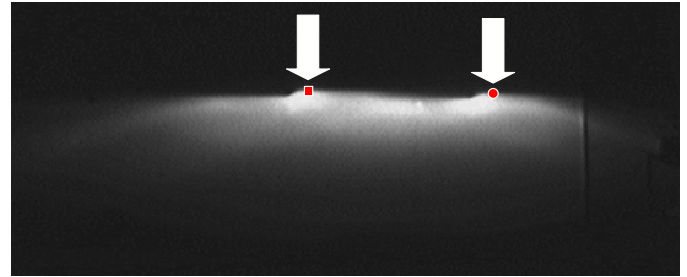


Fig. 9. Cutoff line tracking for two light distributions on a projection surface

Using the camera model from section 6, the tracked points and the known headlamp position, the dynamic inclination angle $\theta_{H,ECUF}$ is estimated. It is compared to the reference angle in figure 10 and reveals a maximum error of 0.25%.

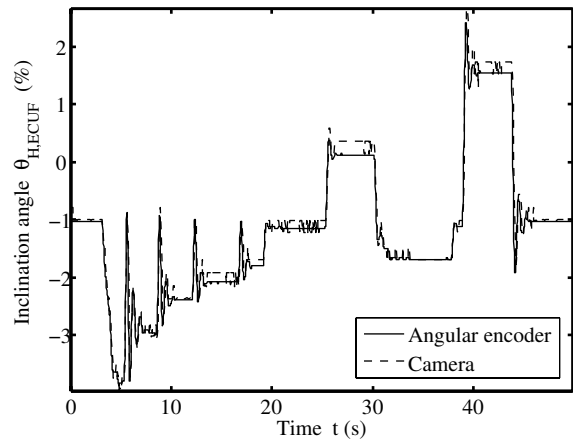


Fig. 10. Measured headlamp inclination

REFERENCES

P. Lehnert. Calist - a lighting tool for designing dynamic headlamp levelling systems. In *FISITA World Automotive Congress*, 2000.

P. Opgen-Rhein and T. Bertram. Development of a dynamic headlamp levelling system using new modelling concepts. In *6th International Symposium on Advanced Vehicle Control (AVEC)*, pages 481–486, Hiroshima/Japan, 2002.

P. Opgen-Rhein, T. Bertram, J. Seuss, and D. Strychik. New challenges in the range of headlamp levelling systems require new development environments. In *5. International Symposium Progress in Automobile Lighting (PAL)*, pages 751–769, Darmstadt, 2003.

O. Schreer. *Stereoanalyse und Bildsynthese*. Springer, 2005.

B. Wördenweber, J. Wallaschek, P. Boyce, and D. D. Hoffmann. *Automotive Lighting and Human Vision*. Springer, 2007.

Z. Zhang. Flexible camera calibration by viewing a plane from unknown orientations. volume 1, page 666. Seventh International Conference on Computer Vision (ICCV'99), 1999.